

## Article

# Modified Ni Nanoparticles as Additives in Various Greases: Assessment of Comparative Performance Potential

Jiabei Wang<sup>1,2</sup>, Hong Zhang<sup>1</sup>, Wenjing Hu<sup>1,3,\*</sup> and Jiusheng Li<sup>1,3,\*</sup> <sup>1</sup> Laboratory for Advanced Lubricating Materials, Shanghai Advanced Research Institute, Chinese Academy of Sciences, Shanghai 201210, China<sup>2</sup> University of Chinese Academy of Sciences, Beijing 100049, China<sup>3</sup> Key Laboratory of Low-Carbon Conversion Science & Engineering, Shanghai Advanced Research Institute, Chinese Academy of Sciences, Shanghai 201210, China

\* Correspondence: huwj@sari.ac.cn (W.H.); lij@sari.ac.cn (J.L.)

**Abstract:** China's rapid industrial development requires more energy consumption based on non-renewable energy resources. The energy consumption caused by unnecessary friction accounts for about 4.5% of the GDP in China. Although grease effectively lubricates machines, lubrication failure may occur under severe conditions. Nanomaterials exhibit intriguing tribological performances and have received much attention regarding lubrication. In this study, oleylamine-modified Ni nanoparticles (OA-Ni) were synthesized and used as lubricant additive in four kinds of commonly used greases: lithium, calcium, composite calcium, and polyurea grease. The OA-Ni were uniformly dispersed in the greases through electromagnetic stirring, ultrasonic vibration, and three-roll grinding. The physicochemical properties and the structure of OA-Ni-doped grease were investigated, while the feasibility of OA-Ni as various grease additives at different contact modes was evaluated by a four-ball friction tester and a UMT-tribolab tester. Tribological tests results revealed that the friction-reducing and anti-wear properties of point-to-point contact were increased by 56.7% and 70.3% in lithium grease, respectively, while those of the point-to-face contact were increased by 59.5% and 68.9% in polyurea grease, respectively. The present work provides not only theoretical guidance of nano nickel modification but also a practical reference for the application of modified nanomaterials to various greases.

**Keywords:** nano-lubrication; modified nanomaterial; multiple greases; tribological properties

**Citation:** Wang, J.; Zhang, H.; Hu, W.; Li, J. Modified Ni Nanoparticles as Additives in Various Greases: Assessment of Comparative Performance Potential. *Lubricants*

2022, 10, 367. <https://doi.org/10.3390/lubricants10120367>

Received: 30 November 2022

Accepted: 15 December 2022

Published: 17 December 2022

**Publisher's Note:** MDPI stays neutral with regard to jurisdictional claims in published maps and institutional affiliations.



**Copyright:** © 2022 by the authors. Licensee MDPI, Basel, Switzerland. This article is an open access article distributed under the terms and conditions of the Creative Commons Attribution (CC BY) license (<https://creativecommons.org/licenses/by/4.0/>).

## 1. Introduction

Due to China's massive manufacturing industry and high energy consumption, the country is known to suffer from a huge waste problem [1]. Over-abrasion and friction are critical factors that contribute to the annual waste caused by the country's mechanical equipment [2,3]; consequently, lubricating is a pivotal technology that will play a huge role in China's industrial development. Lubricating grease, which is crucial to China's industrial lubricant field, is a semi-solid lubricating material composed of thickener and base oil [4]. The lubricating grease widely used in mechanical engineering includes lithium grease (LiG), calcium grease (CaG), composite calcium grease (C-CaG), polyurea grease (PuG), etc. [5]. Compared with lubricating oils, greases are more appropriate in specific situations due to their semi-solid state [6–9]. This conforms to the concept advocated by green chemistry and meets the requirements of modern society for sustainable development [10]; however, the amount of research on high-performance grease in China is significantly lower than the world average, and the up-market is still monopolized by foreign products [11]; therefore, it is imperative to accelerate the development of grease-related research.

The rapid development of modern industry in China constantly requires the transformation of equipment into precise, intelligent versions [12]; thus, the environment of moving parts has become more complex, and increasingly demanding requirements have

been proposed for grease to maintain the regular operation of apparatus and extend the service life of equipment [13]; therefore, conventional lubricant additives cannot suit the demands of present industrial development [14]. With the development of nanotechnology, nanomaterials have emerged as a solution to enhance the tribological characteristics of commercial lubricants to ensure the efficient operation of machines [15]. There was research on nanometer additives in China in the 1990s when the topic of nanomaterial lubrication was raised. Zhang et al. [16] synthesized a molybdenum disulfide ( $\text{MoS}_2$ ) nano cluster and confirmed it features a low-friction coefficient ( $\mu < 0.1$ ) and a great load-carrying ability. Studies have shown that nanoparticle additives possess superior tribological properties compared to traditional solid additives [17,18]. Among them, Ni nanoparticles with magnetism as well as corrosion resistance have been widely researched and used in diverse situations [19,20]. Qiu et al. [21] confirmed the feasibility of Ni nanoparticles as lubricating oil additives in 2001. Plenty of research has also demonstrated the great prospect of Ni nanoparticles and their modified versions in lubrication [22].

Although there have been plenty of studies on modified Ni nanoparticles, most of them are investigated in LiG, and few have focused on their properties in diversified categories of grease, including CaG, C-CaG, and PuG [23,24]; meanwhile, it is well-known that, in a practical situation, the tribological behavior of lubricants cannot truly be limited to a single form of contact because there are many forms of mechanical contact; therefore, it is crucial to simulate the actual conditions with disparate contact forms and investigate the effect of nanomaterials on the tribological behavior of various lubricating greases under disparate contact forms. This is of great guiding significance for the development of nanomaterials additives.

Taking into account the above considerations, oleylamine-modified Ni nanoparticles (OA-Ni) were synthesized for this paper, and four ordinary greases were selected as dispersion systems. The differences in structure and tribological properties of various OA-Ni-doped greases were compared. The lubrication mechanisms were also analyzed to supply academic direction and technical assistance for commercial applications, which has pivotal theoretical significance and practical value.

## 2. Materials and Methods

### 2.1. Materials

In this study, lithium grease (LiG), calcium grease (CaG), composite calcium grease (C-CaG), and polyurea grease (PuG) (Hupai Petroleum Co., Ltd., Ningbo, China) were used as the base greases. Poly alpha olefins (PAO4) were purchased from Formosa Petrochemical Co., Ltd., Taipei, China. Nickel (II) formate dihydrate ( $\text{Ni}(\text{HCOO})_2 \cdot 2\text{H}_2\text{O}$ ), oleylamine (OA), and oleic acid were procured from Shanghai Aladdin Co., Ltd., Shanghai, China. The analytical reagents, titanium butoxide, alcohol, and petroleum ether (PE), were acquired from Sinopharm Chemical Reagent Co., Ltd., Shanghai, China. To ensure easy commercialization, all the raw materials are available in the commercial market without needing further purification.

### 2.2. Preparation of OA-Ni and Doped Greases

#### 2.2.1. Synthesis of OA-Ni

$\text{Ni}(\text{HCOO})_2 \cdot 2\text{H}_2\text{O}$  (1 eq) and oleylamine (2 eq) were added into the round bottom flask and heated to 120 °C with an oil bath under magnetic stirring to obtain a green and transparent Ni formate oleylamine solution. Appropriate amounts of PAO4 and oleic acid (1.8 eq) were added to the solution and heated to 230 °C. The reaction was completed in  $\text{N}_2$  to ensure an anhydrous and anaerobic environment. Finally, after being naturally cooled to room temperature (25 °C), the product was washed with ethanol and centrifuged to obtain nanoparticles. The dried product named OA-Ni was finally acquired after drying for 3 h in a vacuum (Figure 1a).

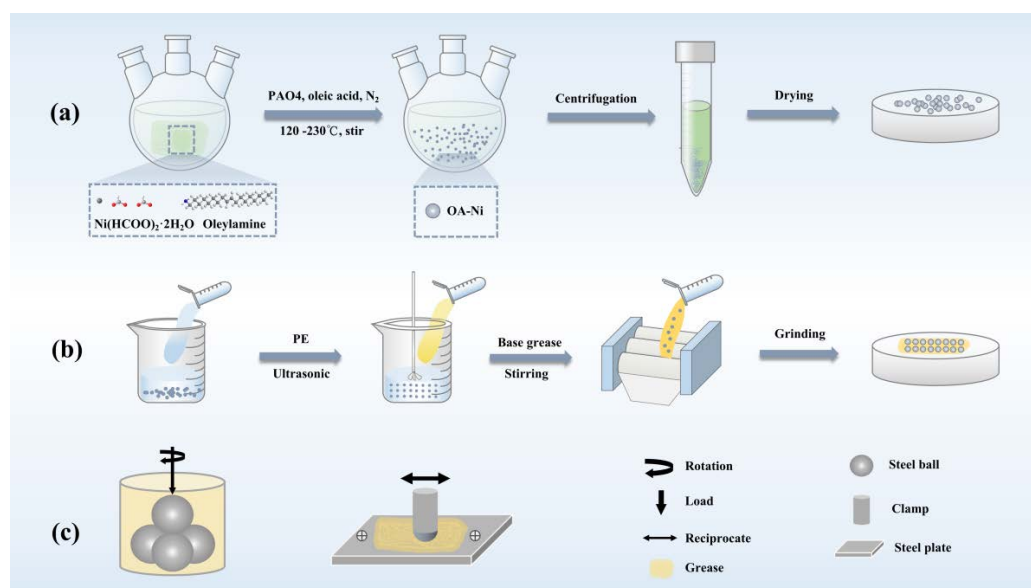


**Figure 1.** The schematic of (a) preparation procedure of OA-Ni and (b) OA-Ni-doped greases; (c) friction contact modes.

### 2.2.2. Preparation of Greases Containing OA-Ni

Four typical greases and OA-Ni nanoparticles were selected to fabricate doped grease. To evenly distribute OA-Ni in all greases, 0.3 wt% OA-Ni nanoparticles were added to four greases, respectively. Each grease sample was dissolved with 15 mL of PE. The mixtures were mechanically stirred at 50 °C until PE was completely evaporated. Subsequently, further dispersion was conducted in the ultrasonic machine for 30 min. Finally, the four greases consistent with OA-Ni were obtained after homogenization using the triple-roller mill three times (Figure 1b). The same degree of grinding was carried out for the pure greases to prevent the additional effects of grinding on the structure and properties.

## 2.3. Physicochemical and Tribological Properties Characterization

### 2.3.1. Physicochemical Characterization Tests

The dropping point, penetrations, and oil-separation rate of pure greases and OA-Ni-doped greases were examined according to national standards. The dropping point of OA-Ni-doped greases was investigated by a DFYF-303 drop-point tester (Dalian Analytical Instrument Co., Ltd., Dalian, China) following GB/T 4929. The penetrations were quantitated by a DFYF-308 grease cone penetrometer (Dalian Analytical Instrument Co., Ltd.) according to GB/T 269. The oil separation was evaluated by the standard GB/T 392. The average data were obtained from three-times tests to confirm dependability.

### 2.3.2. Tribological Properties Tests

The tribological performance of OA-Ni in various greases under point-to-point contact (Figure 1c) was evaluated on the four-ball friction tester (Tianji Automation Co., Ltd., Xiamen, China). Before each experiment, the commercially available steel (GCr15, 12.7 mm, HRC 59–61) balls were cleaned by PE through ultrasonication. Every test was carried out with a load of 196 N, a rotational speed of 1200 r/min, for 120 min at 50 °C. The real-time friction coefficients (COF) were logged on the computer automatically. The optical microscope was used to measure the wear-scar diameter (WSD) of the lower stationary balls to describe the anti-wear property of the greases.

For further investigation of the tribological behavior of diverse greases under point-to-face contact (Figure 1c), the UMT tribometer (UMT-tribolab, Bruker, Billerica, MA, USA) was carried out at a reciprocating stroke of 10 mm, test temperature of 25 °C, frequency of 2 Hz, test period of 1 h, and applied load of 5 N. The lower steel disk (304 stainless steel,

20 mm × 20 mm) slides against the upper steel ball (GCr15 steel, diameter of 8 mm). The UMT tribometer was linked to a computer to record the real-time COF.

## 2.4. Characterization

### 2.4.1. Characterization of OA-Ni and Doped Greases

A transmission electron microscope (TEM, JEOL JEM200, Japan Electronics Corporation, Hiroshima, Japan) and a scanning electron micrograph (SEM, Mira3 XH, Tescan, Brno, Czech) were used to investigate the morphology and agglomeration state of OA-Ni, and the size distribution of the OA-Ni was simultaneously calculated by nano-measure software. X-ray diffraction (XRD, Smart Lab, Rigaku, Tokyo, Japan) and a Fourier transform infrared radiation spectrometer (FTIR, PerkinElmer Spectrum Two) were applied to establish the chemical structure of the OA-Ni nanoparticles.

A polarizing microscope (POM, XP-330C, Caikang Optical Instrument Co., Ltd. Shanghai, China) was adopted to observe the dispersion degree of OA-Ni in the greases. The structural transformation of lubricating grease before and after adding OA-Ni was investigated through SEM. Thickener was obtained by ultrasonics and centrifugation of the solution of grease and PE.

### 2.4.2. Characterization of Worn Surfaces

The surface analysis of the worn surface is a vital way to investigate the lubrication mechanism. Since LiG grease is the most widely used grease in the Chinese market, we took LiG as a representative to study the friction-reducing and anti-wear properties of OA-Ni in various greases. The morphology of the frayed area was studied by white-light interferometer (WLI, Contour GT, Bruker, Billerica, USA) and SEM. Typical elements were investigated with energy-dispersive spectroscopy (EDS, Aztec X-Maxx 80). X-ray photoelectron spectroscopy (XPS, Kratos, AXIS Ultra DLD multifunctional) was used to analyze the chemical state of the target elements.

## 3. Results

### 3.1. Characterization Results of OA-Ni

The morphology and size distribution of nanoparticles is essential to performance, and this was demonstrated in TEM (Figure 2a) and SEM (Figure 2b) images. The prepared OA-Ni nanoparticles were regular spheres with clear edges, which reflect an acceptable degree of agglomeration. The size distribution (Figure 2c) was concentrated between 90–120 nm, mainly 100 nm. The results showed that the OA-Ni nanoparticles were stable, and could maintain structural characteristics in greases, thus, being capable of excellent performance. The crystal structure and chemical structure of OA-Ni are shown in XRD (Figure 2d) and FTIR (Figure 2e). The diffraction peaks at  $44.51^\circ$ ,  $51.85^\circ$ , and  $76.38^\circ$  correspond to (111), (220), and (220) crystal planes of nanoparticles Ni, respectively. The comparison of OA-Ni with the Ni standard card (JCPDS card no. 04-0850) confirms the face-centered cubic (FCC) structure of OA-Ni; additionally, there are no other peaks in the spectrum, indicating that the prepared OA-Ni has high purity. The FTIR spectrum of OA and OA-Ni are shown in Figure 1e, where it can be observed that the peaks located at  $2927\text{ cm}^{-1}$  and  $2880\text{ cm}^{-1}$  are stretching symmetrical tensile vibrations of  $-\text{CH}_3$  and  $-\text{CH}_2$ . The C-H vibration is found at  $1460\text{ cm}^{-1}$ . The vibration peak at  $720\text{ cm}^{-1}$  is attributed to  $-(\text{CH}_2)_n-$  ( $n \geq 4$ ), which proves the existence of long carbon chains. The sharp peak at  $1070\text{ cm}^{-1}$  proves the existence of the C-N stretching vibration bond, and the characteristic peak was also observed in the OA-Ni infrared curve; moreover, the complexation of the Ni cation in OA-Ni leads to the disappearance of the  $-\text{NH}_2$  in OA at  $3200\text{ cm}^{-1}$ . The characterization results confirm that OA was efficaciously grafted on the surface of nanoparticles Ni, which restrict the oxidation and accumulation of nanoparticles Ni. The agglomeration of nanoparticles seriously hinders its performance and even leads to additional wear. Accordingly, it is essential to determine the dispersion of OA-Ni in the doped greases for subsequent tribological performance research. The opaque particles in the POM image (Figure 2f) are

OA-Ni, which are uniformly dispersed without large-scale agglomeration. This indicates that our preparation method resulted in uniform OA-Ni-doped greases.

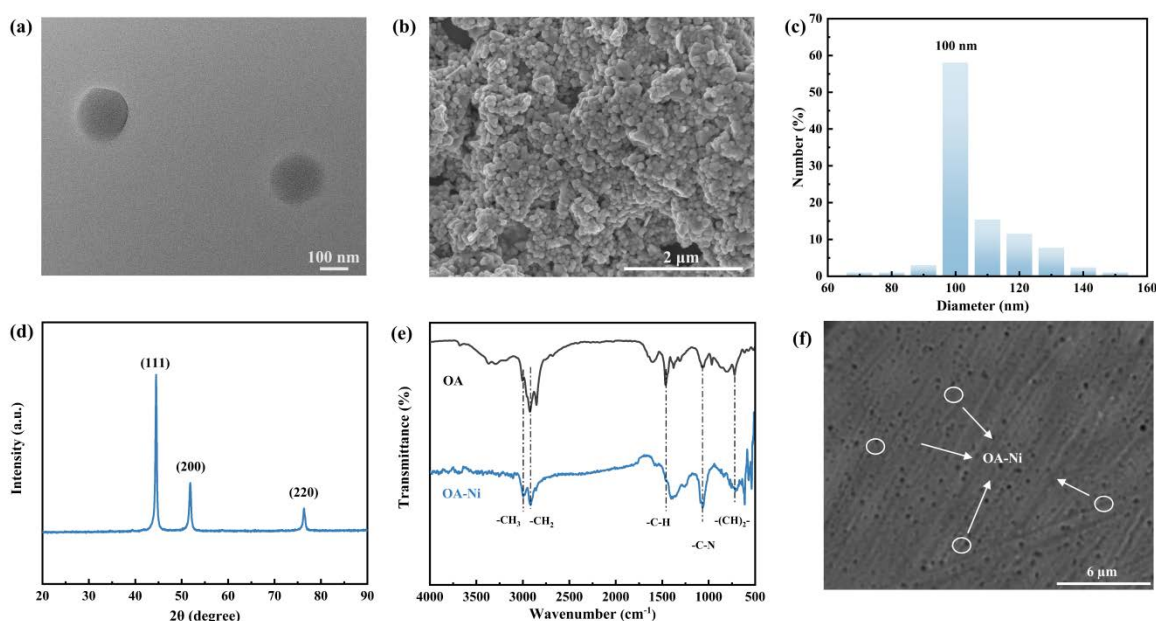


**Figure 2.** Characterization results of OA-Ni nanoparticles: (a) TEM image; (b) SEM image; (c) particle-size distribution; (d) XRD pattern; (e) FTIR spectrum; and (f) dispersion of OA-Ni nanoparticles in grease.

### 3.2. Characterization of Greases

The structure of lubricating grease refers to the physical arrangement of thickener, additive, and base oil. The shape and distribution of thickeners are the key factors affecting the physicochemical and tribological properties of grease; thus, the study of the implication of additives on the thickener structure is significant to further evaluate its lubrication mechanism. SEM images of four greases before and after adding OA-Ni are shown in Figure 3a–h. LiG has long and straight linear fibers, which are closely stacked. The fiber of CaG shows a large bending degree, and it gathers multiple bundles and extends in the same direction. The single fibers of C-CaG are irregular short rods, and the overall shape displays irregular sheets. The long fibers of PuG thickener are interlaced to form a dense network structure. With the introduction of OA-Ni, the uniformly dispersed nanoparticle spheres are clearly visible in the greases; moreover, countless shear planes are formed between OA-Ni nanoparticles, which severely damage the fibers of doped grease in the same grinding operation, thus, leading to the reduction of the length of the thickener and certain damage to the original morphology.

The dropping point, cone penetration, and oil separation correspond to the high-temperature index, hardness index, and colloid stability index of the grease, respectively, which are the necessary application parameters in the industrial field and which are directly affected by the structure and composition of the grease. As shown in Table 1, the difference between the pure greases and the doped greases in the drop point and cone penetration is insignificant; presumably, this is due to the limited OA-Ni content, which is insufficient to constitute a complete construction in doped greases. Interestingly, oil separation displays an apparent difference. The introduction of OA-Ni markedly decreases oil separation. This comparison is related to the structure of the thickener (Figure 3a–h). It is speculated that the damage of OA-Ni to the tight thickener network diminishes the binding capacity of fibers to the base oil; thus, the oil will seep from OA-Ni-doped greases under the pressure [25]; moreover, it is crucial for the grease lubrication to continuously release a proper oil to form the continuous lubricating film, otherwise, it will cause excessive wear or the reduction of the grease's service life.

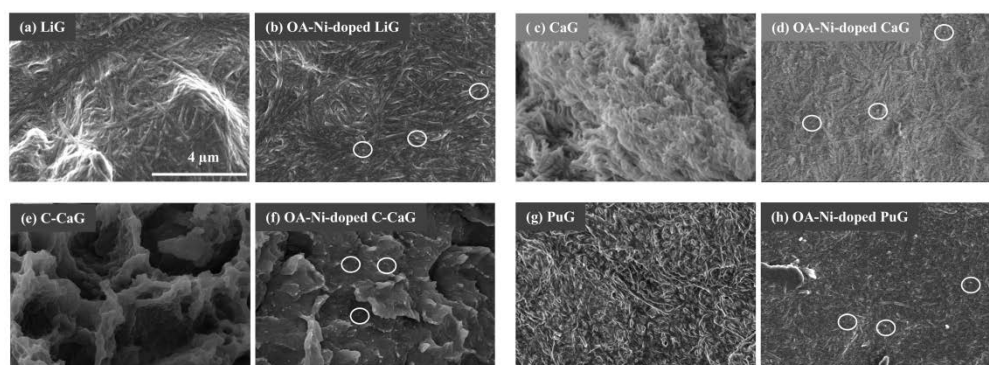


**Figure 3.** Characterization results: SEM images of (a) LiG, (b) OA-Ni-doped LiG; (c) CaG, (d) OA-Ni-doped CaG; (e) C-CaG; (f) OA-Ni-doped C-CaG; (g) PuG, and (h) OA-Ni-doped PuG. In the white circle are OA-Ni nanoparticles of the doped greases. All images have the same magnification.

**Table 1.** The physical characterization results of greases.

	National Standard	LiG	OA-Ni-Doped LiG	CaG	OA-Ni-Doped CaG	C-CaG	OA-Ni-Doped C-CaG	PuG	OA-Ni-Doped PuG
Dropping point (°C)	GB/T 4929	188.3	187.0	172.9	170.2	177.4	177.9	182.5	186.3
Penetration	GB/T 269	365.6	368.2	305.3	309.5	338.1	340.6	420.5	434.9
Cone penetration (0.1 mm)	GB/T 392	0.6	1.7	0.2	0.8	0.4	1.3	1.1	2.1

### 3.3. Results of Tribological Tests

The universal application fields of grease focus on mechanical moving parts, such as gears and bearings, which consists of point-to-point contact and point-to-face contact; thus, the appropriate selection of test modules is essential to simulate the performance of grease under actual working conditions. Under point-to-point contact, the average COF and WSD of greases are shown in Figure 4a,b. The introduction of OA-Ni shows a constructive effect in all four types of grease. In the comparison with the LiG, CaG, C-CaG, and PuG, the OA-Ni significantly improved the friction-reduction performance by 25.0%, 6.3%, 29.1%, and 7.5%, with the anti-wear performance increased by 28.4%, 2.7%, 14.6%, and 7.5%, respectively. The concern is that LiG and C-CaG show the most sensitive response to the addition of OA-Ni; in contrast, the CaG and PuG samples have undergone only insignificant changes.

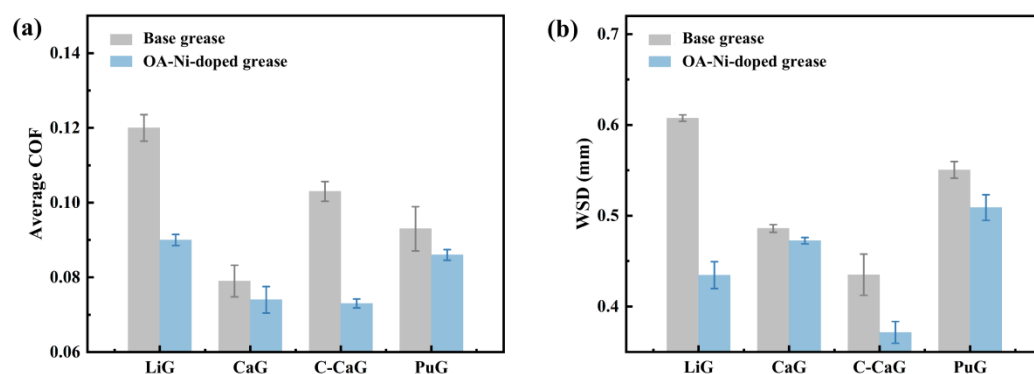


**Figure 4.** Tribological properties of the various pure grease and OA-Ni-doped grease under point-to-point contact: (a) average COF; and (b) WSD.

Figure 5a,b shows the average COF and worn surfaces of greases under point-to-face contact. Obviously, the friction-reduction properties of PuG are significantly reduced (30.2%) due to the addition of OA-Ni among the various greases tested, while other types of grease show inconspicuous change, and even the friction coefficient of CaG has increased

slightly (2.2%). The rubbing produces conspicuous wide hollows and serious disruption on the wear region by pure PuG grease lubrication, while a glossy scar with a mild crease was discovered from OA-Ni-doped PuG grease.

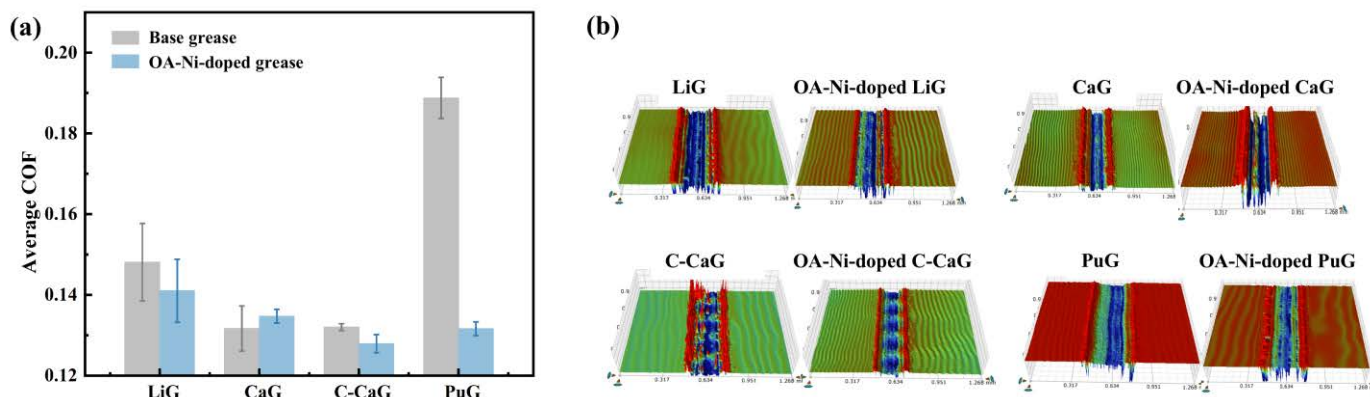


**Figure 5.** Tribological properties of the various pure greases and OA-Ni-doped greases under point-to-face contact: (a) average COF; and (b) WLI morphologies of wear scar.

### 3.4. SEM and EDS Analysis of Worn Surface

The characterization of the rubbing area is useful for further studying the anti-wear mechanism of OA-Ni. As shown in Figure 6a–h, compared with the SEM morphologies of OA-Ni-doped greases, the striking grooves, abrasions, and abrasives are found on the rubbing area lubricated by the pure greases [26]. The introduction of OA-Ni significantly reduces the degree of wear, while the area turns flat and smooth. The obvious distinction between the pure greases and OA-Ni-doped greases is that OA-Ni enhances the abrasion resistance of various greases. The distribution of key elements of the rubbing area lubricated by the OA-Ni-doped LiG is shown in Figure 6i. It is evident that the worn scar is evenly covered with N element and Ni element, which originate from the OA-Ni. This verifies the existence of the deposited film [27]; moreover, considering the worn surfaces are washed with PE before the analysis of the elements, the solid film formed by OA-Ni is stable.

The elemental and morphological characterization of the rubbing area confirmed the filling and polishing effect of OA-Ni. OA-Ni is deposited in the contact surface grooves to increase its smoothness and flatness and, then, form a solid physical layer with low shear stress; meanwhile, the sphere-like OA-Ni converts sliding friction into rolling friction, thus, preventing direct contact between the friction area and hindering the incidence of extreme situations.

### 3.5. XPS Analysis of the Worn Surface

XPS analysis verifies the existence of chemical reaction film in the contact interface and clarifies the chemical states. The XPS spectra of the worn scar lubricated with LiG and OA-Ni-doped LiG are shown in Figure 7. The peak at 284.6 eV is indicative of C in the air. The peak at 288.5 eV is indicative of C=O [28]. The binding of O1s at 530.7 eV prove that  $\text{Fe}_3\text{O}_4$  is generated in the contact surface [29]. The peak of 529.6 eV and 557.7 are indicative of NiO and Ni. The peak at 532.4 eV is indicative of the oxygen in the NO. The peaks of Fe2p at 710.1 eV and 723.74 eV correspond to  $\text{Fe}_3\text{O}_4$  and  $\text{Fe}_2\text{O}_3$ , respectively. The peak that appears at 855.9 eV is attributed to  $\text{Ni}_2\text{O}_3$  [30], while the peaks of other Ni2p all prove that the chemical reaction occurred in the friction process of OA-Ni-doped LiG.

Considering the above discussion, it is confirmed that OA-Ni-doped greases generate a surface protective film through tribochemical reactions, which are composed of Ni, NiO,  $\text{Ni}_2\text{O}_3$ , ferrites, and compounds containing C-O bonding.

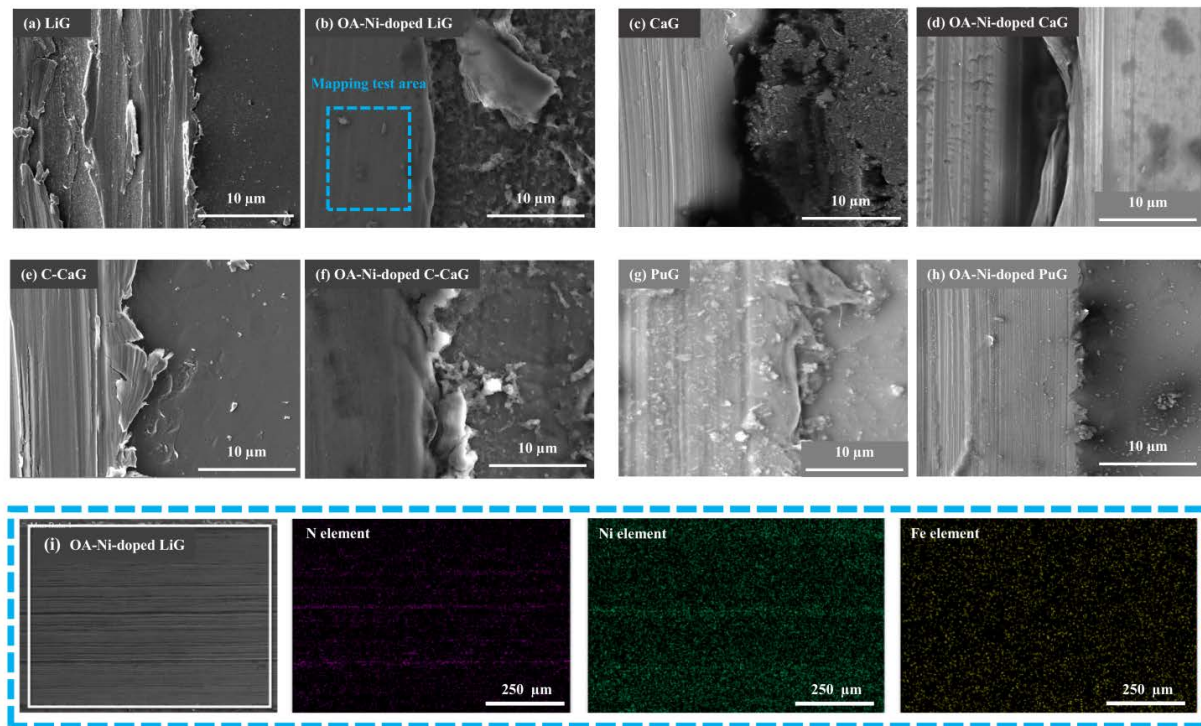


**Figure 6.** Characterization of worn scar and its edge: SEM images of (a) LiG, (b) OA-Ni-doped LiG; (c) CaG, (d) OA-Ni-doped LiG; (e) C-CaG; (f) OA-Ni-doped C-CaG; (g) PuG, (h) OA-Ni-doped PuG; and (i) EDS mapping images of the surfaces lubricated by OA-Ni-doped LiG.

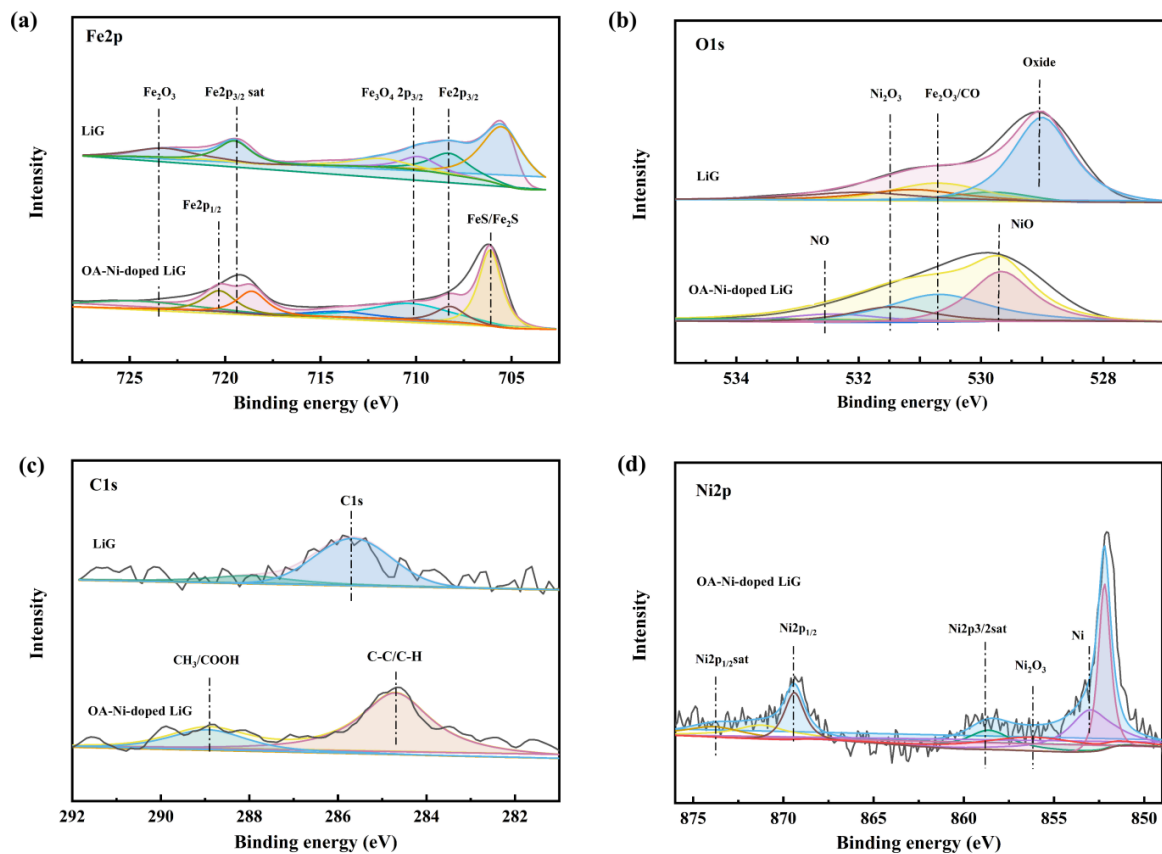


**Figure 7.** XPS spectra of (a) Fe2p; (b) O1s; (c) C1s; and (d) Ni2p on the worn scars of steel balls lubricated by LiG and OA-Ni-doped LiG after four-ball tests.

### 3.6. Possible Mechanism

The tribological data infer that OA-Ni produces a marked effect on the lubricating properties of LiG, C-CaG, and PuG, but not on CaG. It is speculated that the tribological behavior is related to the structural and physicochemical properties of the four greases. The thickeners of LiG and C-CaG are composed of straight fibers with irregular staggered distribution (Figure 3a,e), which provide countless gaps in the intersection. The added OA-Ni is exposed through the gaps rather than be bound to the fibers (Figure 3b,f); thus, it has the opportunity to function in a small contact area and form a lubricating film (point-to-point contact, Figure 4a,b). The directionally growing fiber bundles are formed in CaG (Figure 3c), which leads to an increased hardness of the grease (Table 1). It is difficult for OA-Ni to function once it enters the thickener bundle; moreover, the decreased hardness and the low binding capacity are produced by the thin fibers (Figure 3g) in PuG. OA-Ni in the PuG is easily introduced into the friction interface with the release of base oil (Figure 3h); thus, OA-Ni-doped PuG has the best lubrication performance under strong shear (point-to-face contact, Figure 5a,b). In conclusion, the possible lubrication mechanism of OA-Ni in diverse greases is speculated according to the above results (Figure 8):

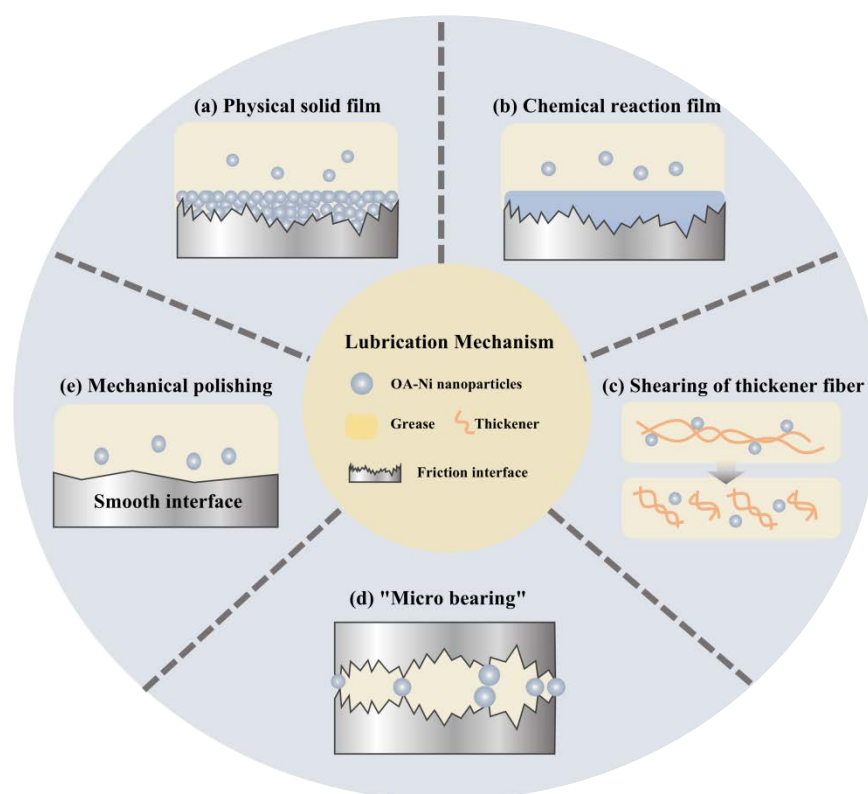


**Figure 8.** Schematic of the lubrication mechanism of OA-Ni nanoparticles as an additive in various greases.

1. Physically solid film (Figure 6). Attributed to the high specific surface, the nanoparticle Ni with high adsorption capacity and OA organic chain is adsorbed in the boundary lubrication zone and easily converted into adsorption film [31];
2. Chemical reaction film (Figures 6 and 7). The organic chain on OA-Ni reacts with the friction material, while, to a certain extent, the high temperature promotes the chemical reaction; this temperature originates from the thermal energy induced by the friction. Accordingly, the chemical reaction film is formed on the contact area [32];
3. Shearing of the thickener fiber (Figure 3). The thickener structure is easily damaged by the shearing of OA-Ni, thus, decreasing the ability to bind to the additive and base oil. The released oil and additives form a continuous oil film and reaction film that play a lubricating role [33];

4. Micro bearing effect (Figure 6). The sphere-like OA-Ni converts the sliding friction into rolling friction; in such a manner, direct contact is prevented during the friction process, which is akin to “micro bearings” on the friction area [34];
5. Polishing effect (Figure 6). OA-Ni mechanically polishes the nanoscale protrusion of the rough surface, while a smooth surface increases the friction area and, thus, avoids severe wear.

#### 4. Conclusions

In this paper, the comparative performance potential and lubrication mechanism of various greases with oleylamine-modified Ni nanoparticle additives are studied experimentally. Crucial conclusions are listed as follows:

- (1) The introduction of OA-Ni has a constructive effect on all four types of greases. Under point-to-point conduct, LiG and C-CaG exhibit the most sensitive response to OA-Ni. In contrast, CaG and PuG samples demonstrate only insignificant responses. Under point-to-face conduct, the tribological properties of PuG show the most obvious improvement, while the performance of other greases is not significantly enhanced;
- (2) The lubrication mechanism of OA-Ni offers the following benefits: it generates a physically solid film and a chemical-reaction film, it shears the thickener fiber, and it uses mechanical polishing as “micro bearing”. The synergy of these functions greatly broadens working conditions and prolongs serving life in comparison with pure grease.

**Author Contributions:** Conceptualization, J.W., H.Z., W.H. and J.L.; methodology, J.W., H.Z. and J.L.; validation, J.W., H.Z. and J.L.; formal analysis, J.W., H.Z. and W.H.; investigation, J.W. and H.Z.; data curation, J.W. and H.Z.; writing—original draft preparation, J.W.; writing—review and editing, J.W., W.H. and J.L.; supervision, J.W., W.H. and J.L. All authors have read and agreed to the published version of the manuscript.

**Funding:** The authors would like to thank the Youth Innovation Promotion Association, CAS (2019288), the Strategic Priority Research Program of the Chinese Academy of Sciences (XDA21021202), and the Foundation of Key Laboratory of Low-Carbon Conversion Science & Engineering, Shanghai Advanced Research Institute, Chinese Academy of Sciences (grant nos. KLLCCSE-202203Z, SARI, and CAS) for financial support for this work.

**Institutional Review Board Statement:** Not Applicable.

**Informed Consent Statement:** Not Applicable.

**Data Availability Statement:** Not Applicable.

**Conflicts of Interest:** The authors declare no conflict of interest.

#### References

1. He, B.; Liu, S.; Zhao, X.; Liu, J.; Ye, Q.; Liu, S.; Liu, W. Dialkyl dithiophosphate-functionalized gallium-based liquid-metal nanodroplets as lubricant additives for antiwear and friction reduction. *ACS Appl. Nano Mater.* **2020**, *3*, 10115–10122. [[CrossRef](#)]
2. Li, Z.; He, Q.; Du, S.; Zhang, Y. Effect of few layer graphene additive on the tribological properties of lithium grease. *Lubr. Sci.* **2020**, *32*, 333–343. [[CrossRef](#)]
3. Yu, H.; Xu, Y.; Shi, P.; Wang, H.; Wei, M.; Zhao, K.; Xu, B. Microstructure, mechanical properties and tribological behavior of tribofilm generated from natural serpentine mineral powders as lubricant additive. *Wear* **2013**, *297*, 802–810. [[CrossRef](#)]
4. Furukawa, H.; Cordova, K.E.; O’Keeffe, M.; Yaghi, O.M. The chemistry and applications of metal-organic frameworks. *Science* **2013**, *341*, 1230444. [[CrossRef](#)]
5. Rahman, M.; Hayat, T.; Khan, S.A.; Alsaedi, A. Entropy generation in sutterby nanomaterials flow due to rotating disk with radiation and magnetic effects. *Math. Comput. Simul.* **2022**, *197*, 151–165. [[CrossRef](#)]
6. Bakunin, V.N.; Suslov, A.Y.; Kuzmina, G.N.; Parenago, O.P. Synthesis and application of inorganic nanoparticles as lubricant components—a review. *J. Nanopart. Res.* **2004**, *6*, 273–284. [[CrossRef](#)]
7. Krawiec, S. On the mechanism of the synergistic effect of PTFE and copper in a lithium grease lubricant. *Ind. Lubr. Tribol.* **2011**, *63*, 171. [[CrossRef](#)]
8. Sanchez, C.; Chen, Y.; Parkinson, D.Y.; Liang, H. In situ probing of stress-induced nanoparticle dispersion and friction reduction in lubricating grease. *Tribol. Int.* **2017**, *111*, 66–72. [[CrossRef](#)]

9. Mariño, F.; López, E.R.; Arnos, Á.; González Gómez, M.A.; Piñeiro, Y.; Rivas, J.; Alvarez-Lorenzo, C.; Fernández, J. ZnO nanoparticles coated with oleic acid as additives for a polyalphaolefin lubricant. *J. Mol. Liq.* **2022**, *348*, 118401. [[CrossRef](#)]
10. Zhao, J.; Yang, G.; Zhang, C.; Zhang, Y.; Zhang, S.; Zhang, P. Synthesis of water-soluble Cu nanoparticles and evaluation of their tribological properties and thermal conductivity as a water-based additive. *Friction* **2019**, *7*, 246–259. [[CrossRef](#)]
11. Guo, J.; Cheng, J.; Tan, H.; Sun, Q.; Yang, J.; Liu, W. Constructing a novel and high-performance liquid nanoparticle additive from a Ga-based liquid metal. *Nanoscale* **2020**, *12*, 9208–9218. [[CrossRef](#)] [[PubMed](#)]
12. Salah, N.; Abdel-Wahab, M.S.; Alshahrie, A.; Alharbi, N.D.; Khan, Z.H. Carbon nanotubes of oil fly ash as lubricant additives for different base oils and their tribology performance. *RSC Adv.* **2017**, *7*, 40295–40302. [[CrossRef](#)]
13. Hu, J.; Wang, C.; Zhang, P.; Zhang, S.; Zhang, Y. Diisooctyl sebacate-containing Nickel nanoparticles for lubrication of steel sliding parts under magnetic fields. *ACS Appl. Nano Mater.* **2021**, *4*, 7007–7016. [[CrossRef](#)]
14. Maksimova, Y.M.; Shakhmatova, A.S.; Ilyin, S.O.; Pakhmanova, O.A.; Lyadov, A.S.; Antonov, S.V.; Parenago, O.P. Rheological and tribological properties of lubricating greases based on esters and polyurea thickeners. *Rheol. Tribol. Prop.* **2018**, *58*, 1064–1069. [[CrossRef](#)]
15. Kumara, C.; Luo, H.; Leonard, D.N.; Meyer, H.M.; Qu, J. Organic-modified silver nanoparticles as lubricant additives. *ACS Appl. Mater. Interfaces* **2017**, *9*, 37227–37237. [[CrossRef](#)]
16. Zhang, Z.; Zhang, J.; Xue, Q. Synthesis and characterization of a molybdenum disulfide nanocluster. *J. Phys. Chem.* **1994**, *98*, 12973–12977. [[CrossRef](#)]
17. Meng, Y.; Su, F.; Chen, Y. Nickel/Multi-walled carbon nanotube nanocomposite synthesized in supercritical fluid as efficient lubricant additive for mineral oil. *Tribol. Lett.* **2018**, *66*, 134. [[CrossRef](#)]
18. Reinert, L.; Varenbery, M.; Mücklich, F.; Suárez, S. Dry friction and wear of self-lubricating carbon-nanotube-containing surfaces. *Wear* **2018**, *406–407*, 33–42. [[CrossRef](#)]
19. Ahmad, U.; Raza Naqvi, S.; Ali, I.; Saleem, F.; Taqi Mehran, M.; Sikandar, U.; Juchelková, D. Biolubricant production from castor oil using iron oxide nanoparticles as an additive: Experimental, modelling and tribological assessment. *Fuel* **2022**, *324*, 124565. [[CrossRef](#)]
20. Tóth, Á.D.; Szabó, Á.I.; Leskó, M.Z.; Rohde-Brandenburger, J.; Kuti, R. Tribological Properties of the Nanoscale Spherical Y<sub>2</sub>O<sub>3</sub> Particles as Lubricant Additives in Automotive Application. *Lubricants* **2022**, *10*, 28. [[CrossRef](#)]
21. Qiu, S.; Zhou, Z.; Dong, J.; Chen, G. Preparation of Ni nanoparticles and evaluation of their tribological performance as potential additives in Oils. *ASME J. Tribol.* **2001**, *123*, 441–443. [[CrossRef](#)]
22. Shu, J.; Harris, K.; Munavirov, B.; Westbroek, R.; Leckner, J.; Glavatskih, S. Tribology of polypropylene and Li-complex greases with ZDDP and MoDTC additives. *Tribol. Int.* **2018**, *118*, 189–195. [[CrossRef](#)]
23. Li, D.; Xie, Y.; Yong, H.; Sun, D. Surfactant-assisted preparation of Y<sub>2</sub>O<sub>3</sub>-stabilized ZrO<sub>2</sub> nanoparticles and their tribological performance in mineral and commercial lubricating oils. *RSC Adv.* **2017**, *7*, 3727–3735. [[CrossRef](#)]
24. Singh, Y.; Rahim, E.A.; Singh, N.K.; Sharma, A.; Singla, A.; Palamanit, A. Friction and wear characteristics of chemically modified mahua (*madhuca indica*) oil based lubricant with SiO<sub>2</sub> nanoparticles as additives. *Wear* **2022**, *508–509*, 204463. [[CrossRef](#)]
25. Ye, X.; Wang, J.; Fan, M. Evaluating tribological properties of the stearic acid-based organic nanomaterials as additives for aqueous lubricants. *Tribol. Int.* **2019**, *140*, 105848. [[CrossRef](#)]
26. Wu, H.; Wei, D.; Hee, A.C.; Huang, S.; Xing, Z.; Jiao, S.; Huang, H.; Jiang, Z. The influence of water-based nanolubrication on mill load and friction during hot rolling of 304 stainless steel. *Int. J. Adv. Manuf. Technol.* **2022**, *121*, 7779–7792. [[CrossRef](#)]
27. Szabó, Á.I.; Tóth, Á.D.; Leskó, M.Z.; Hargitai, H. Investigation of the Applicability of Y<sub>2</sub>O<sub>3</sub>-ZrO<sub>2</sub> spherical nanoparticles as tribological lubricant additives. *Lubricants* **2022**, *10*, 152. [[CrossRef](#)]
28. Wang, X.; Wei, X.; Zhang, J.; Li, R.; Hua, M.; Wang, W. formation of nanocrystallized structure in worn surface layer of T10 steel against 20CrMnTi steel during dry rubbing. *J. Nanomater.* **2016**, *2016*, 4631851. [[CrossRef](#)]
29. Thampi, A.D.; Prasanth, M.A.; Anandu, A.P.; Sneha, E.; Sasidharan, B.; Rani, S. The effect of nanoparticle additives on the tribological properties of various lubricating oils—Review. *Mater. Today Proc.* **2021**, *47*, 4919–4924. [[CrossRef](#)]
30. Bhushan, B.; Israelachvili, J.N.; Landman, U. Nanotribology: Friction, wear and lubrication at the atomic scale. *Nature* **1995**, *374*, 607–616. [[CrossRef](#)]
31. Gundarneeya, T.P.; Vakharia, D.P. Performance analysis of journal bearing operating on nanolubricants with TiO<sub>2</sub>, CuO and Al<sub>2</sub>O<sub>3</sub> nanoparticles as lubricant additives. *Mater. Today Proc.* **2021**, *45*, 5624–5630. [[CrossRef](#)]
32. Zhang, R.; Liu, X.; Guo, Z.; Cai, M.; Shi, L. Effective suger-derived organic gelator for three different types of lubricant oils to improve tribological performance. *Friction* **2020**, *8*, 1025–1038. [[CrossRef](#)]
33. Radulescu, A.V.; Radulescu, I. Rheological models for lithium and calcium greases. *Mechanics* **2016**, *59*, 67.
34. Ali, Z.A.A.A.; Takhakh, A.M.; Al-Waily, M. A review of use of nanoparticle additives in lubricants to improve its tribological properties. *Mater. Today Proc.* **2022**, *52*, 1442–1450. [[CrossRef](#)]